Synthesis and EPR characterisation of triphenylmethane derivatives carrying *N*-*tert*-butyl nitroxide radical moieties: use of the diradical as a ligand for a complex with $Mn^{II}(hfac)_2$

Daniela Carmen Oniciu, Kenji Matsuda and Hiizu Iwamura *

*Institute for Fundamental Research in Organic Chemistry, Kyushu University,
6-10-1 Hakozaki, Higashi-Ku, Fukuoka 812-81, Japan*

Oxidation of the tris(hydroxylamine) 3 with various oxidants has been monitored by EPR spectroscopy and found to show stepwise formation of the corresponding mononitroxide radical 4, dinitroxide radical 5 and trinitroxide radical 6, which was finally converted into the quinonoid diradical 8. The robust triplet nature of diradical 8 was corroborated by its effective magnetic moment of 2.7 μ_B at 300 K. When mixed with bis(hexafluoroacetylacetonato)manganese(II), $Mn(hfac)_2$, diradical 8 gave black–violet solids 9 of formula $[Mn(hfac)_2]_3 \cdot 8_2$. The temperature dependence of the reciprocal of the molar susceptibility of the complex indicated a ferromagnetic interaction with a Curie constant $C = 7.86$ emu K mol^{-1} and a Weiss temperature $\theta = 87.5$ K. At 5 K, hysteresis with a coercive force of 17 Oe and a remaining magnetisation of 910 emu G mol^{-1} was observed, confirming the phase transition to a magnet.

Introduction

Various approaches to the study of organic molecular magnets fall into four chief categories.[1] The first is the survey and design of molecular crystals of organic free radicals, only a limited number of which have been shown to undergo a transition to spin-ordered phases at temperatures not higher than 1.5 K. The second is based on the fact that electron spins can couple more strongly within polyradical, polycarbene, and polynitrene molecules. However, while they can be extended to large systems in principle, the numbers of parallel spins are, so far, limited to 18 and macroscopic alignment of spins has not been achieved yet.[2] Charge-transfer salts as a third leading principle proved to be important in that they opened up this field and often have high magnetic phase-transition temperatures. Many of them are, however, unstable in air. The fourth and most viable alternative is the self-assemblage and organisation of organic radicals by means of coordination to magnetic metal ions.[3] Nitroxide radicals† and bis(hexafluoroacetylacetonato)-manganese(II), $Mn(hfac)_2$, play a versatile role in such complexation reactions and many molecular magnets arising from these sources have been reported.[3,4] The highest magnetic phase-transition temperature (T_c) reported is 46 K.[3c] The advantage of this strategy is that the size and sign of the exchange coupling and the dimensions of the magnetic structures can be controlled *a priori* by choosing magnetic metal ions and designing organic ligands. The appropriate degree of flexibility and the symmetry of the ligands control the magnetic property of the resulting magnetic materials.[3,4] Thus design and synthesis of new *tert*-butylnitroxide radicals are expected to realise even higher T_c.

We now report the synthesis of a novel quinonoid dinitroxide radical, which has three ligating sites in a triangular disposition and may be used as a ligand in the complexation with $Mn(hfac)_2$, to give a complex expected to display relevant magnetic properties.

Results and discussion

Synthesis

Tris(*p*-bromophenyl)methanol 1 was obtained by reacting ethyl *p*-bromobenzoate with 2 mol equiv. of *p*-bromophenylmagnesium iodide as described in the literature.[5,6] Tris(*p*-bromophenyl)methane 2 was prepared in good yields by reducing 1 with chlorotrimethylsilane according to a procedure described for benzylic alcohols.[7] The tribromo compound 2 was subsequently treated with *tert*-butyllithium[8] and 2-methyl-2-nitrosopropane to give the tris(hydroxylamine) 3 (Scheme 1).

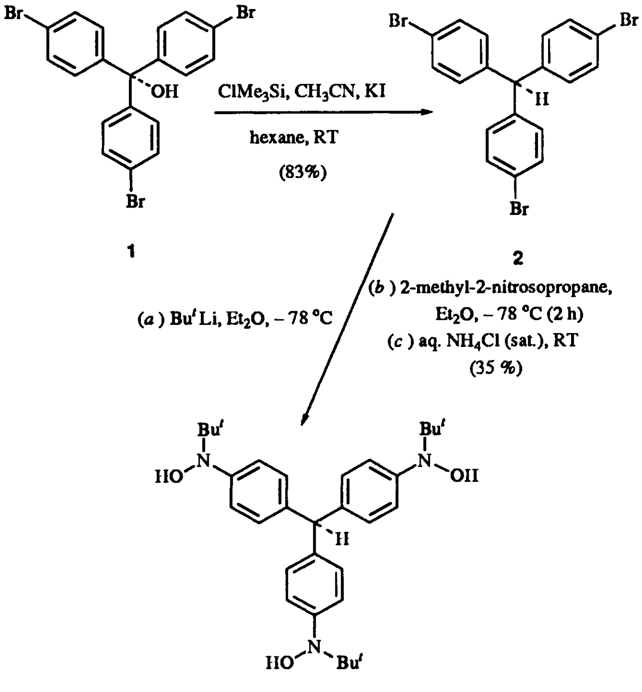

Scheme 1

The oxidation of 3 with freshly prepared silver(I) oxide occurred stepwise, and the first two stages of the oxidation were evidenced by monitoring the reaction in sealed and degassed EPR tubes (Scheme 2). Mononitroxide radical 4 was confirmed as the initial oxidation product (Fig. 1). After 1.5 h, the changes in the EPR spectrum showed the formation of dinitroxide radical 5 (Fig. 2), which was further oxidised to trinitroxide radical 6 (Fig. 3).

---

† IUPAC recommended name: aminoxyl.

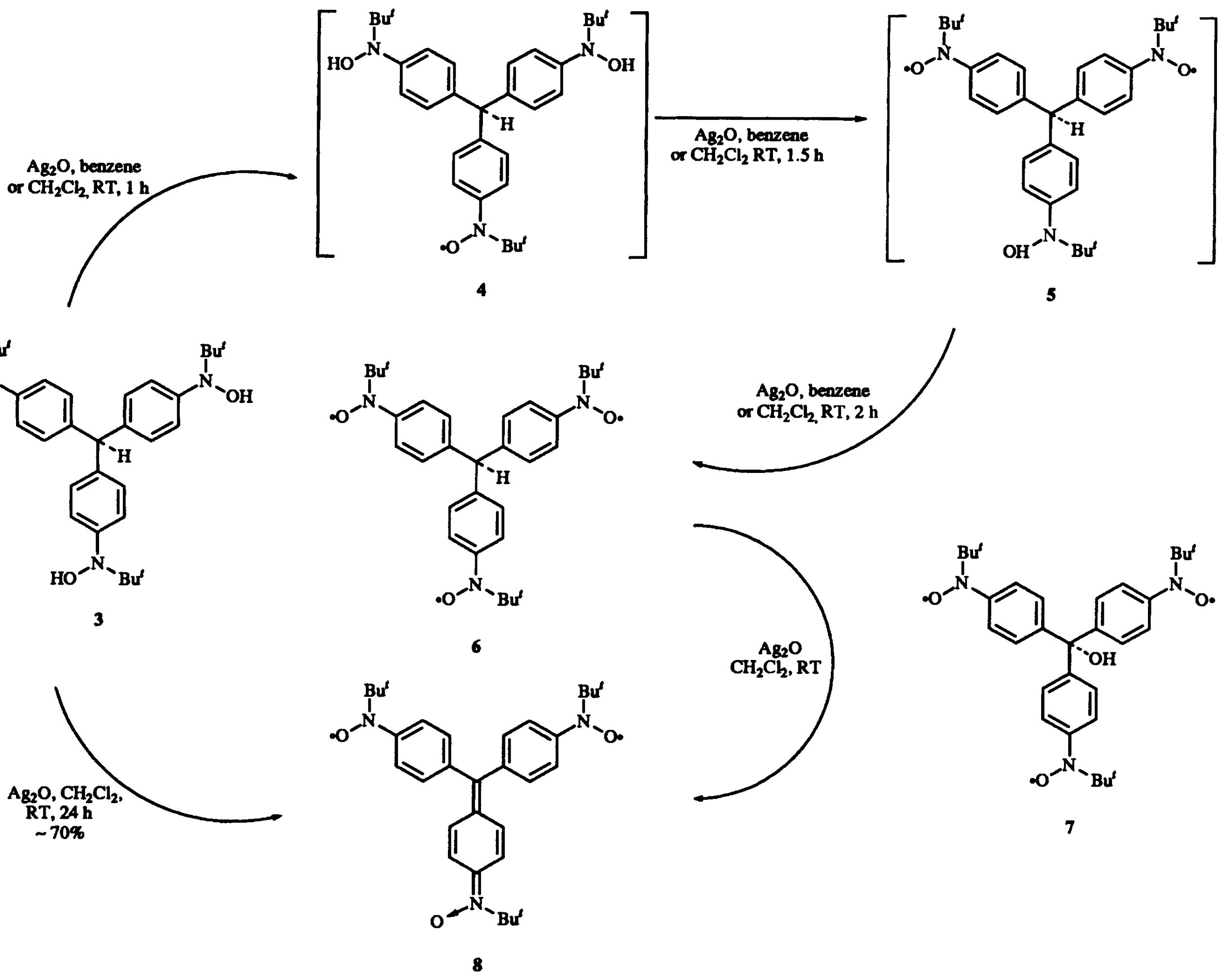

Scheme 2

In preparative experiments, **3** was oxidised by contact either with lead dioxide or silver(I) oxide for 2 h to give the trinitroxide radical **6**. In view of the structural similarity of **6** with tris[*p*-(*N*-ylooxy-*tert*-butylamino)phenyl]methanol **7**,[9] which has been purified and characterised, we thought compound **6** was likely to be a stable crystalline solid. However, contrary to expectations, it was readily oxidised further to give the quinonoid dinitroxide radical **8**.

The transformation of the triradical **6** into the diradical **8** was effected by using a large excess of oxidant. When the oxidation was performed in benzene for more than 2 h, a mixture of **6** and **8** was obtained. When methylene chloride was used as the solvent and silver(I) oxide or MCPBA as the oxidant, **8** was obtained almost exclusively after 24 h; TLC showed only a trace of **6**, which was completely oxidised to **8** during the work-up. The reaction could be monitored by EPR spectroscopy.

Diradical **8** was reacted with $Mn(hfac)_2$ in various solvents: diethyl ether, methylene chloride and mixtures of methylene chloride and heptane. The reaction was performed under conditions already described in literature.[3] A black–violet complex **9** was obtained and shown to have the expected composition $[Mn(hfac)_2]_3 \cdot \mathbf{8}$ by elemental analysis (Scheme 3).

Structural studies of radicals 4, 5 and 6

The EPR spectrum, consisting of a triplet of octets, obtained at the initial stage of the oxidation [Fig. 1(*a*)] was simulated by use of the hyperfine couplings with nitrogen (a_N = 12.89 G, 1 N), *ortho* (a_H = 2.00 G, 2 H) and *meta* (a_H = 0.88 G, 2 H) phenyl ring hydrogens, and a benzylic hydrogen (a_H = 0.85 G, 1 H) as shown in Fig. 1(*b*) and is consistent with an *N*-centred monoradical **4**, rather than a *C*-centred triarylmethyl. The observed distortion of the spectrum and humps between the triplets may be due to the presence of diradicals as described below.

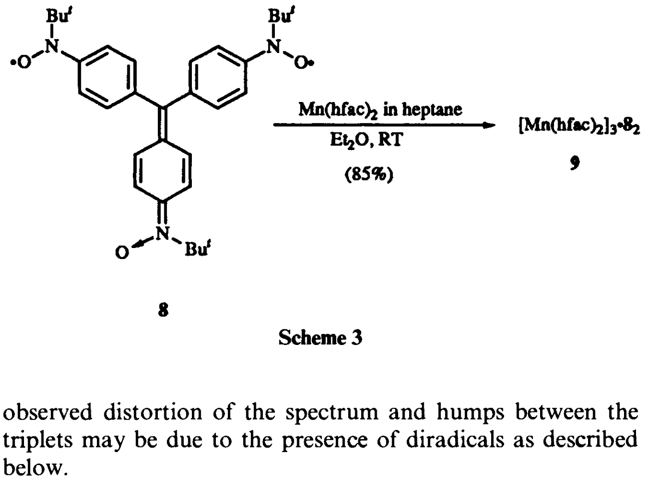

Scheme 3

The EPR spectrum reproduced in Fig. 2 was assigned to diradical **5**. The hyperfine structure (a_N = 6.56 G, 2 N, $a_{ortho\text{-}H}$ = 1.96 G, 2 H, $a_{meta\text{-}H}$ = 0.88 G, 2 H, and $a_{benzylic\text{-}H}$ = 0.84 G, 1 H) of the spectrum revealed a characteristic linewidth alternation due to the intermediate rate of the exchange between the two unpaired electrons relative to the nitrogen hyperfine coupling or to fluctuation of the latter.[10] The rather small exchange coupling parameter *J* must be ascribed to the sp^3 hybridised central carbon atom separating the two π-radical moieties.

The EPR spectrum of the triradical **6** recorded at room temperature consisted of a septet (Fig. 3), indicating that the unpaired electrons interact with three equivalent nitrogen atoms and therefore $|J|$ is much greater than the hyperfine

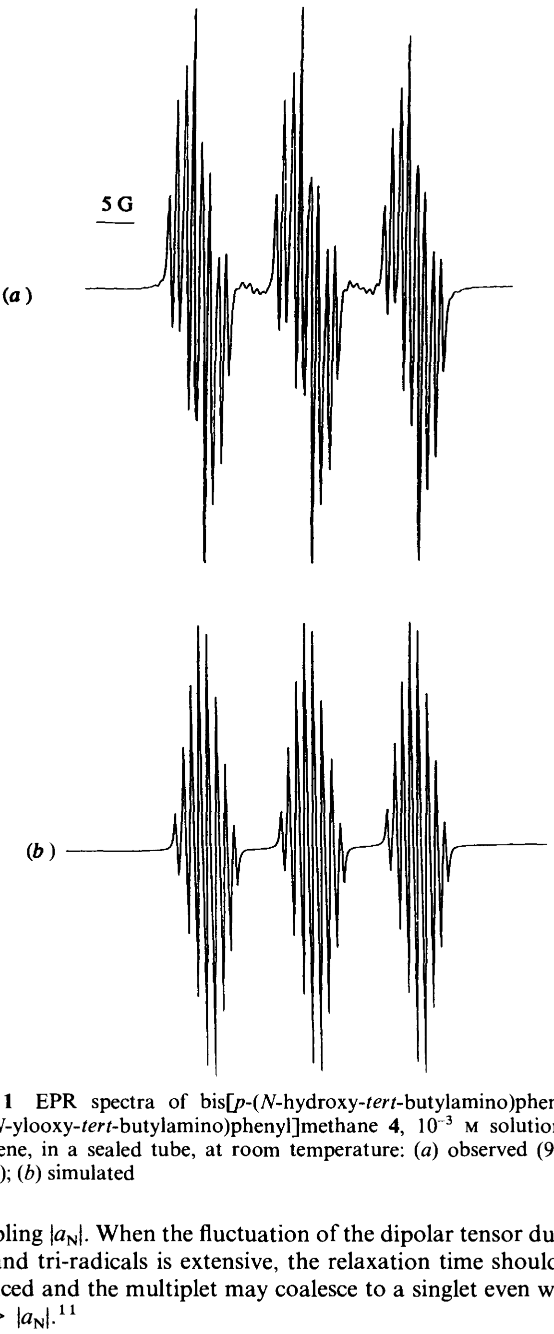

Fig. 1 EPR spectra of bis[*p*-(*N*-hydroxy-*tert*-butylamino)phenyl]-[*p*-(*N*-ylooxy-*tert*-butylamino)phenyl]methane **4**, 10^{-3} M solution in benzene, in a sealed tube, at room temperature: (*a*) observed (9.419 GHz); (*b*) simulated

coupling $|a_N|$. When the fluctuation of the dipolar tensor due to di- and tri-radicals is extensive, the relaxation time should be reduced and the multiplet may coalesce to a singlet even when $|J| > |a_N|$.[11]

The triradical **6** had a lifetime of more than 10 days in degassed solution, but not in the crystalline state. The *g*-factor ($g = 2.005$) and the hyperfine coupling constant ($a_N = 4.40$ G, 2 N) are similar in magnitude to those of tris[*p*-(*N*-ylooxy-*tert*-butylamino)phenyl]methanol **7** ($a_N = 4.00$ G, 2 N),[9] which was, however, stable in the crystalline state. EPR spectra of these radicals did not change in shape at room temperature down to the freezing point of the solvent, excluding conformational equilibria.

Structure assignment for diradical 8

A hydrogen abstraction reaction from the central carbon of the triarylmethane is suggested for the product of complete oxidation of the tris(hydroxylamine) **3** or further oxidation of triradical **6**. The tetraradical was not detected by EPR measurements; the observed spectrum is interpreted in terms of the quinonoid resonance structure **8** of higher thermodynamic stability as shown below. The UV–VIS spectrum showed several bands characteristic of the conjugated systems (see the Experimental).[12]

The molar magnetic susceptibility χ for powder samples of diradical **8** was investigated at 5000 and 10000 Oe in the temperature range 5–300 K on a SQUID susceptometer. The effective magnetic moment μ_{eff} was evaluated to be 2.7 μ_B at 5000 G at 300 K. The theoretical μ_{eff} value is 2.83 μ_B for the pure triplet species, whereas a diradical with degenerate triplet and singlet states should have μ_{eff} 2.45 μ_B. The observed value is much higher than the latter and shows that diradical **8** is a robust triplet in that the energy gap between the ground triplet and excited singlet states is not much smaller than kT at 300 K. As the temperature is lowered, the μ_{eff} values decrease continuously and sharply at 20 K, suggesting the presence of a strong antiferromagnetic intermolecular interaction, if not dimerisation by chemical recombination, between the radical centres.[13] The magnetic impurity of a solid sample of **8** suggested by a slightly lower room-temperature μ_{eff} value than the theoretical one may also be due to this strong antiferromagnetic interaction.

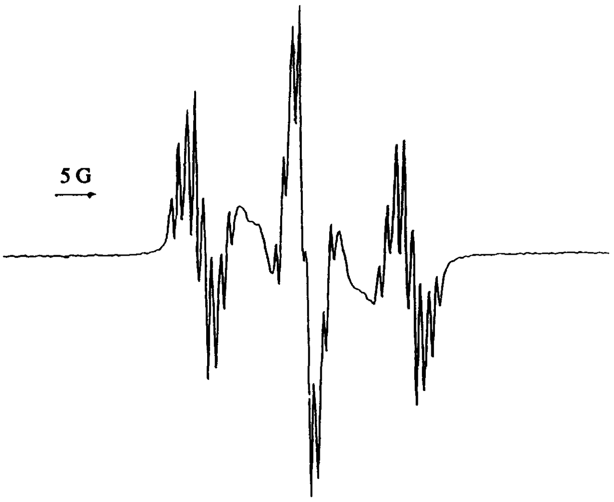

Fig. 2 EPR spectrum of *p*-(*N*-hydroxy-*tert*-butylamino)phenyl-bis[*p*-(*N*-ylooxy-*tert*-butylamino)phenyl]methane **5** in benzene at 253 K (9.433 GHz)

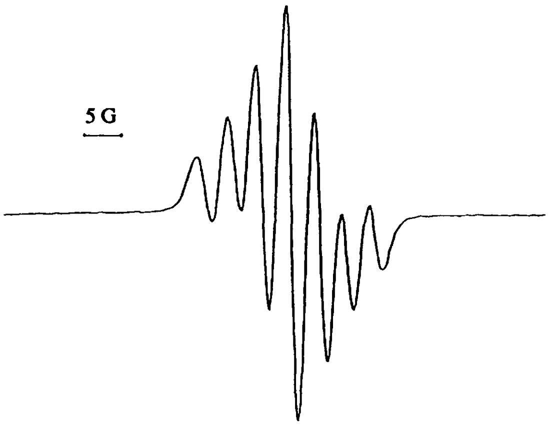

Fig. 3 EPR spectrum of tris[*p*-(*N*-ylooxy-*tert*-butylamino)phenyl]-methane **6** in benzene at room temperature (9.433 GHz)

The EPR spectrum of **8** recorded in a degassed 2-methyltetrahydrofuran solution revealed hyperfine splittings due to two nitrogen atoms and *ortho*- and *meta*-hydrogens as reproduced in Fig. 4(*a*). Linewidth alternation similar to that of the dinitroxide **5** was again observed.

Operationally there are two extreme structures possible for the diradical **8**. One has a C_3, or nearly C_3, axis of symmetry with the rate of exchange of the two unpaired electrons among the three nitrogen atoms being much faster than the hyperfine coupling a_N [eqn. (1)]. This should have produced a seven-line EPR spectrum due to coupling between these nitrogen atoms. A precedent for such fast exchange and/or resonance can be found in Yang's diradical,[14] which has a triplet ground state and shows coupling with six equivalent ring hydrogens *meta* to the

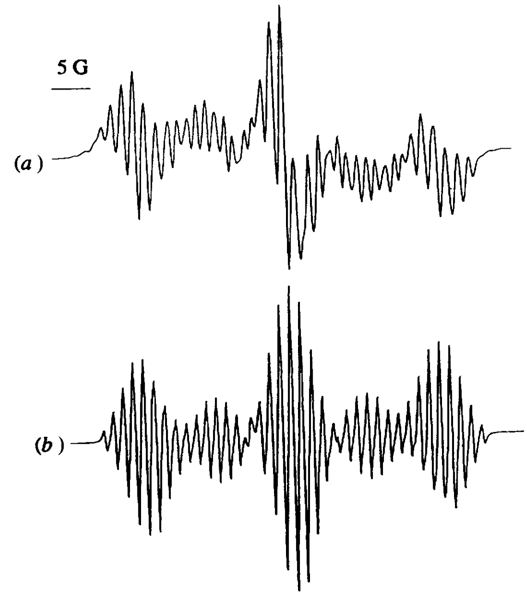

Fig. 4 EPR spectra of 4-{bis[*p*-(*N*-ylooxy-*tert*-butylamino)-phenyl]methylene}cyclohexa-2,5-dienone *N*-tert-butylimine *N*-oxide **8**, recorded for a solution 10^{-3} M in 2-methyltetrahydrofuran: (*a*) experimental spectrum, at room temperature (9.414 GHz); (*b*) simulated spectrum

radical centres. Therefore a D_3 or D_{3h} structure is suggested and, indeed, the latter was observed experimentally by X-ray diffraction. A similar phenomenon, $|J| \gg |a_N|$, is found in the less symmetrical Kurreck diradical.[15] The other possibility would be one fixed quinonoid structure, at least on the EPR timescale. The observed five-line EPR spectrum due to coupling with two nitrogen atoms for **8** is more consistent with this bond localisation. The two *p*-(*N*-ylooxy-*tert*-butylamino)phenyl groups are not equivalent with respect to the nitrone group. Rotation of the aryl groups around the methylene carbon would generate a number of conformers, which would contribute to the fluctuation of the nitrogen hyperfine coupling and the consequent linewidth alternation.[10] Simulation of EPR spectrum of **8** was performed [Fig. 4(*b*)] by assuming that the observed spectrum originated from the sum of the two kinds of the species: two *p*-(*N*-ylooxy-*tert*-butylamino)phenyl groups are nearly coplanar to the nitrone group in one species (**8a**) and one *p*-(*N*-ylooxy-*tert*-butylamino)phenyl groups is twisted out of the plane of the nitrone group in the other (**8b**) (Fig. 5). **8a** has the hyperfine coupling constants, nitroxide (a_N = 6.30 G, 2 N) and nitrone (a_N = 0.85 G, 1 N) nitrogen, *ortho* (a_H = 1.68 G, 2 H) and *meta* (a_H = 0.84 G, 2 H) phenyl ring hydrogens. In **8b** the two spins are independent and may be regarded as a sum of 1 : 1 **8b** (**A**) and **8b** (**B**) [**8b** (**A**): nitroxide (a_N = 12.40 G, 1 N) and nitrone (a_N = 0.86 G, 1 N) nitrogen, *ortho* (a_H = 1.68 G, 2 H) and *meta* (a_H = 0.84 G, 2 H) phenyl ring hydrogens; **8b** (**B**): nitroxide (a_N = 12.40 G, 1 N), *ortho* (a_H = 1.68 G, 2 H) and *meta* (a_H = 0.84 G, 2 H) phenyl ring hydrogens]. When **8a** and **8b** were assumed to be 1 : 4, reproduction of the observed spectrum was reasonable as shown in Fig. 4(*b*).

At temperatures between 250–150 K, the five groups of lines were no longer evident (Fig. 6), but the collapse into three lines [Fig. 6(*c*)] occurred at the freezing temperature of the solvent (CH_2Cl_2), which did not allow us to calculate rotational barriers. Unfortunately, the low stability of diradical **8** has made impossible an X-ray determination of the molecular structure, as a supporting evidence of these considerations.

The dipolar interaction between the two radical centres is weak, as the EPR spectrum showed a broad and little-structured signal at cryogenic temperatures in 2-methyltetrahydrofuran matrix [Fig. 6(*d*)]. The spectral width, as a measure of the zero-field splitting parameter 2*D*, is 140 G, and the *g*-facto is 2.0043. The Δm_s = 2 transitions for the triplet species a about 1600 G were not evident.

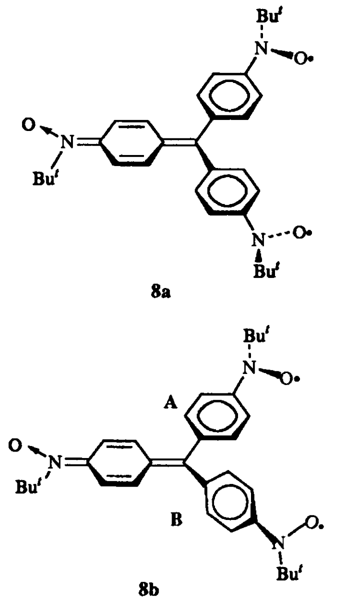

Fig. 5 Two conformers **8a** and **8b** used in simulation

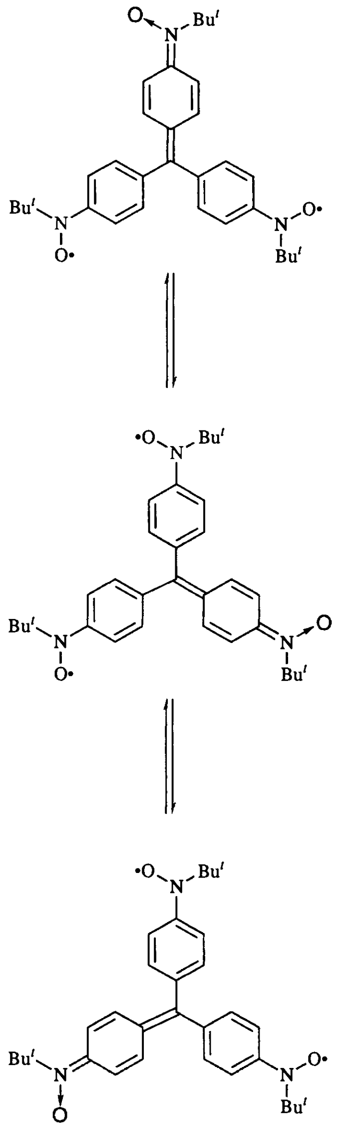

(1)

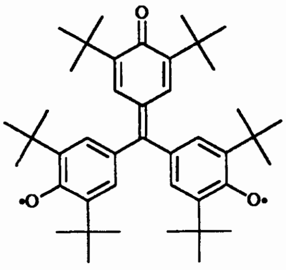

Yang's diradical

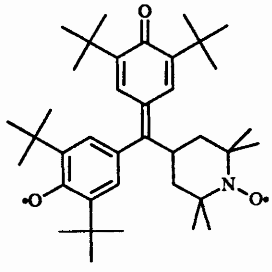

Kurreck's diradical

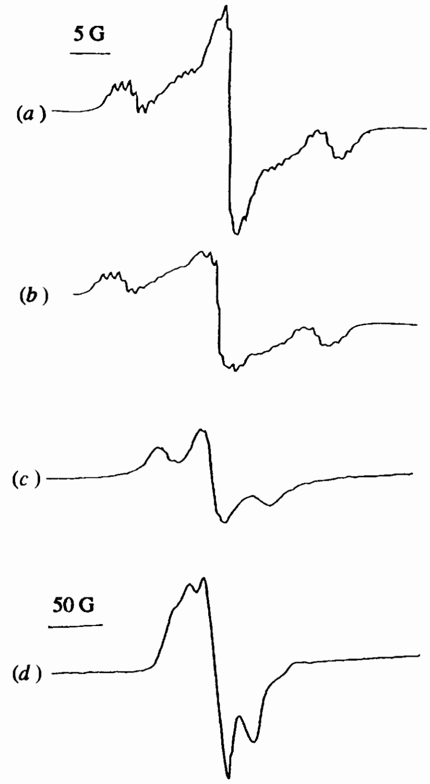

Fig. 6 EPR spectra of 4-{bis[*p*-(*N*-ylooxy-*tert*-butylamino)-phenyl]methylene}cyclohexa-2,5-dienone *N*-*tert*-butylimine *N*-oxide **8**, recorded for a solution 10^{-3} M in 2-methyltetrahydrofuran, at different temperatures (*a*) at 250 K (9.403 GHz); (*b*) at 200 K (9.402 GHz); (*c*) at 150 K (9.408 GHz); (*d*) at 8.5 K (9.411 GHz)

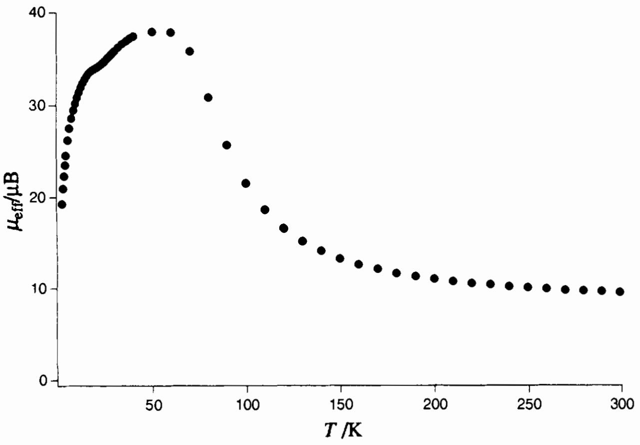

Fig. 7 Temperature dependence of the effective magnetic moment m_{eff} of neat crystals of the manganese complex $[Mn(hfac)_2]_3 \cdot \mathbf{8}_2$ **9**, measured at 50 mT

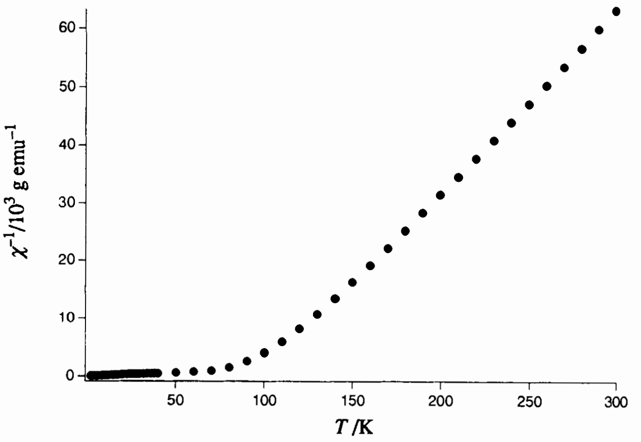

Fig. 8 Temperature dependence of $1/\chi$ of neat crystals of the manganese complex $[Mn(hfac)_2]_3 \cdot \mathbf{8}_2$ **9**, measured at 50 mT

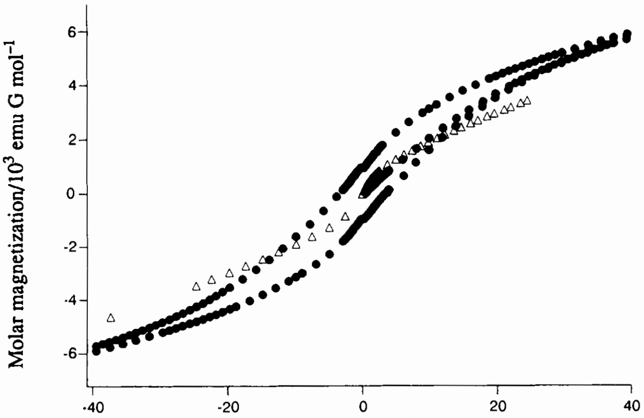

Fig. 9 Field dependence of the magnetisation of neat crystals of $[Mn(hfac)_2]_3 \cdot \mathbf{8}_2$ **9**, measured at 5 K (●) and 50 K (△)

Magnetic properties of complex 9

The paramagnetic susceptibility of $[Mn(hfac)_2]_3 \cdot \mathbf{8}_2$ (**9**) was measured on a SQUID susceptometer using a microcrystalline sample of the complex at 500 Oe in the temperature range 2–300 K. When the data were analysed in terms of the Curie–Weiss relationship (Fig. 7), the Curie constant *C* and Weiss temperature θ were determined to be $C = 7.86$ emu K mol^{-1} and $\theta = +87.5$ K (Fig. 8). The μ_{eff} value of the complex was computed to be 10.5 μ_B at 300 K and the two spins in diradical **8** are in a triplet state at 300 K as mentioned above. A theoretical μ_{eff} value of 11.0 μ_B was derived when the manganese and triplet radical spins are independent. This accounts quite nicely for the observed value of 10.5 μ_B.

The paramagnetic susceptibility that accounts for a strong ferromagnetic interaction can be explained as follows. The interaction between the nitroxide radical and the manganese ion is antiferromagnetic. Within the ligand, the spins on nitroxide radicals are ferromagnetically coupled due to the topological symmetry. The system as a whole is ferrimagnetically ordered. From the Weiss temperature, this material has the potential of showing a phase transition at 87.5 K. The highest μ_{eff} value was 38 μ_B, observed in the temperature range 40–65 K. This value indicates that, as a result of extending the correlation length, the ordering of the spins in this sample extends over *ca.* 5 units on average at 40–65 K.

The field dependence of the magnetisation was studied over the temperature range 5–50 K (Fig. 9). At 5 K, hysteresis was observed, with coercive forces of 17 Oe and a remaining magnetisation of 910 emu G mol^{-1}, confirming the phase transition to a magnet. The magnetic order is lost at 50 K, when the hysteresis curve was no longer observed; at 60 K, the curve became linear. The hysteresis curve at 5 K strongly suggests that long-range ferrimagnetic order exists.

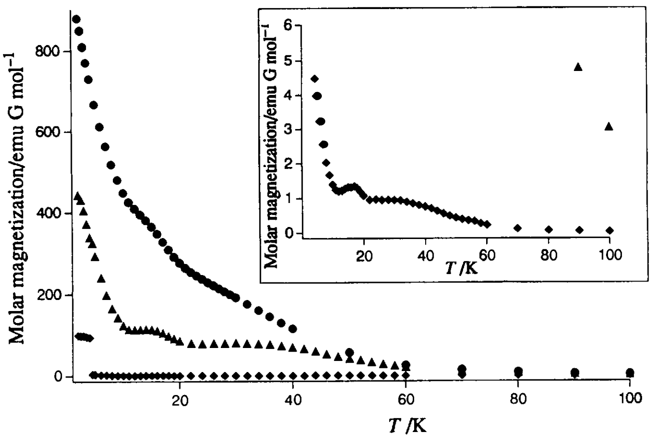

Fig. 10 Temperature dependence of magnetisation of neat crystals of the manganese complex $[Mn(hfac)_2]_3{\cdot}8_2$ **9** at 0.5 mT: (●) field-cooled magnetisation; (▲) zero-field-cooled magnetisation; (◆) remnant magnetisation. Inset: expansion of the remnant magnetisation plot

Several molar magnetisation *versus* temperature plots are shown in Fig. 10. Field-cooled magnetisation (FCM) was measured at 5 Oe by cooling a micro-crystalline sample of complex **9** from 300 K to 2 K. Zero-field-cooled magnetisation (ZFCM) was measured at a magnetic field of 5 Oe, on warming a microcrystalline sample of complex **9** from 2 K to 300 K, immediately after cooling it in a magnetic field of 0 Oe. Remnant magnetisation (REM) was measured on warming a microcrystalline sample of complex **9** in a magnetic field of 0 Oe, after cooling it in a magnetic field of 5 Oe. All three data collections showed the occurrence of a brief invariance of the magnetisation at *ca.* 80, 20 and 10 K, clearly showing the magnetic ordering, with phase transition at 80 K.

The field dependence of magnetisation (Fig. 9) reveals that magnetisation did not level off at 1 T, but the saturation magnetisation should not be much greater than the 6×10^3 emu G mol^{-1} observed at 1 T. Considering the theoretical saturation magnetisation (M_s) value of 6.1×10^4 for complex **9**, the observed value at 1 T corresponds to *ca.* 10% and the experimental M_s is suggested to be significantly lower than the theoretical value. Since the complex **9** is chemically pure, the unsatisfactory M_s value may be interpreted in terms of inhomogeneity in the crystal structure of the complex.

The coordination state of the manganese complex **9** which shows a Weiss temperature of 87.5 K is very intriguing. If the isolation of this compound in a pure state could be achieved, it would lead to a very interesting high-T_c molecular magnetic material.

Conclusions

A new example of a molecular-based magnetic material $[Mn(hfac)_2]_3{\cdot}8_2$, **9** is envisaged, featuring the quinonoid dinitroxide radical **8** as a ligand.

The diradical structure of the ligand **8** was confirmed by SQUID experiments, and the simulation of the EPR spectrum at room temperature showed the existence of different conformers whose overlapped simulated spectra fit the experimental spectrum.

The magnetic properties of the complex **9** were investigated by SQUID experiments. A Curie temperature of 87.5 K was found, as well as a rapid increase of the magnetisation around 80 K. The temperature of the phase transition is unusually high for a molecular magnet.

Experimental

^1H and ^{13}C NMR spectra were recorded on a JEOL GX-270 instrument. IR spectra were obtained on a Hitachi I-5040 spectrometer. ^1H and ^{13}C NMR complete assignments were obtained by using ^1H–^{13}C HETCOR and attached proton test (APT). UV–VIS spectra were recorded on a Hitachi U-3300 spectrophotometer. EPR measurements were made on a Bruker ESP 300E spectrometer. Cryogenic experiments were performed in MTHF matrices at 9 K in the EPR cavity. Temperatures were controlled by an Air Products LTD-3-110 cryogenic temperature controller. The cryostat was maintained at high vacuum by means of a diffusion/rotary pump set. Mass spectra were obtained with a JEOL JMS-SX/SX102A instrument. Melting points are not corrected. Magnetic susceptibilities of the microcrystalline samples were measured with a Quantum Design MPMS2 SQUID system.

Diethyl ether and tetrahydrofuran (THF) used in the reactions were distilled, under a dry nitrogen atmosphere, from sodium–benzophenone ketyl prior to use. 2-Methyltetrahydrofuran (MTHF) used in magnetic measurements was purified by successive distillation from lithium aluminium hydride under nitrogen and from sodium–benzophenone ketyl under nitrogen. All reactions were performed under an atmosphere of dry nitrogen. Anhydrous sodium sulfate was used as a drying agent.

All reactions were monitored by TLC carried out on 0.2 mm Merck silica gel plates (60F-254) using UV light as the detector. Column chromatography was performed on silica gel G60 (Merck, 70–230 mesh) or neutral alumina (ICN, activity grade I). Elemental analyses were performed for stable solid materials. High resolution mass spectra were measured when elemental analysis was not applicable.

EPR experiments were performed in sealed tubes after three freeze–thaw cycles, using various solvents (methylene chloride, benzene and MTHF). The results were not dependent on the nature of the solvent, except for temperatures lower than their freezing points.

Tris(*p*-bromophenyl)methanol (1)

Compound **1** was obtained according to the literature procedure:[5] yield 33% (lit., 29%); mp 130–131 °C (lit., 131 °C).

Tris(*p*-bromophenyl)methane (2)

Compound **2** was obtained according to the literature procedure:[7] yield 83% (lit., 80%); mp 116 °C (lit.,[6] 115 °C).

Tris[*p*-(*N*-hydroxy-*tert*-butylamino)phenyl]methane (3)

The tribromo compound **2** (0.52 g, 1.1 mmol) in Et_2O (20 ml), at −78 °C, was treated with *tert*-butyllithium (7 equiv., 3.4 ml solution 1.7 M in pentane) for 3 h. 2-Methyl-2-nitrosopropane (0.34 g, 3.85 mmol) in Et_2O (20 ml), was added to the slurry solution. The reaction was monitored by TLC, and stopped when no more triphenylmethane was detected (about 2 h). The reaction mixture was allowed to warm to room temperature, and H_2O (50 ml) was added. Additional Et_2O was needed (about 50 ml) for the work-up. The aqueous layer was separated, and the organic layer was washed with sat. NH_4Cl (5×50 ml), and dried. The solvent was evaporated off *in vacuo*, and the residue was chromatographed on silica gel, using as solvents *n*-hexane for high R_f impurities, then *n*-hexane–CH_2Cl_2 (5:1) for the main product. The first fraction eluted was bis[*p*-(*N*-hydroxy-*tert*-butylamino)phenyl]phenylmethane, and the second was the desired product. The tris(hydroxylamine) **3** was recrystallised from toluene–CH_2Cl_2, then from CH_2Cl_2–*n*-hexane: pink solid, yield 35%; mp 137–138 °C; R_f(CH_2Cl_2–Et_2O 3:1) 0.28; δ_H(270 MHz; DMSO) 1.30 (27 H, br s, CH_3), 5.65–5.80 (1 H, m, C*H*Ar), 7.15–7.25 (6 H, m, *ortho*-CH), 7.30–7.45 (6 H, m, *meta*-CH), 8.48 (3 H, br s, N-OH); δ_C(75 MHz; DMSO) 26.0 (9 C, CH_3), 54.3 (1 C, *C*HAr), 59.1 (3 C, *C*-CH_3), 124.1 (6 C, *ortho*-CH), 127.8 (6 C, *meta*-CH), 139.8 (3 C, *C*–CH), 148.6 (3 C, N–C); Calc. for $C_{31}H_{44}N_3O_3$ (MH^+): 506.3383. Found: 506.3379.

Tris[*p*-(*N*-ylooxy-*tert*-butylamino)phenyl]methane (6)

The tris(hydroxylamine) **3** (50 mg, 0.1 mmol) in various solvents (50 ml), was treated with Ag_2O (110 mg), at −78 °C, after which the temperature was raised to 10 °C. After 2 h, the oxidant was filtered off, and the solvent was removed under nitrogen. Red crystals were obtained, which are not stable for more than three days. Attempts to purify this product by column chromatography or recrystallisation failed; complex mixtures were obtained, in which the diradical **8** was the major component. Red crystals, yield 85%; mp 115–117 °C; R_f(CH_2Cl_2–Et_2O 3:1) 0.8; λ_{max}/nm (ε/dm^3 mol^{-1} cm^{-1}): 300 (25 700), 309 (30 200); EPR (room temperature, solution 10^{-3} M in CH_2Cl_2): septet (1:3:6:7:6:3:1), a_N 4.47 G, *g*-factor 2.0050; Calc. for $C_{31}H_{41}N_3O_3$ (MH^+): 503.3148. Found: 503.3137.

4-{Bis[*p*-(*N*-ylooxy-*tert*-butylamino)phenyl]methylene}cyclohexa-2,5-dienone *N*-*tert*-butylimine *N*-oxide (8)

The tris(hydroxylamine) **3** (50 mg, 0.1 mmol) in CH_2Cl_2 (50 ml) was treated with Ag_2O (300 mg), at −78 °C, after which the temperature was raised to 10 °C. After 24 h, the oxidant was filtered off, and the solvent was removed under nitrogen. The product was purified by recrystallisation from diethyl ether, but was not stable enough for us to obtain a good elemental analysis. The purity of crystalline samples was reduced to less than 50% within two weeks at −20 °C. Red–purple crystals, yield 70%; mp 67–71 °C (decomp.); λ_{max}/nm (ε/dm^3 mol^{-1} cm^{-1}): 300 (25 000), 309 (31 800), 377 (17 950), 461.5 (24 000), 553.5 (20 400); EPR (room temperature, solution 10^{-3} M in MTHF): coupling constants indicated in the text, *g*-factor 2.0041.

Complex [Mn(hfac)$_2$]$_3$·**8**$_2$ (9)

The hydrated manganese complex Mn(hfac)$_2$·2H_2O (76 mg, 0.15 mmol) in *n*-heptane (50 ml) was refluxed with a Dean–Stark condenser, until dehydrated. The solution was cooled to room temperature, and the stoichiometric amount of diradical **8**, in a solution prepared as indicated above, was added in one portion. The solvent was removed under nitrogen: black–violet crystals, yield 85%; mp 176–178 °C (decomp.) (Found: C, 45.9; H, 3.9; N, 3.5. Calc. for $C_{92}H_{84}F_{36}Mn_3N_6O_{18}$: C, 45.8; H, 3.5; N, 3.5%); λ_{max}/nm (ε/dm^3 mol^{-1} cm^{-1}): 308.5 (55 000), 461.5 (32 000), 552 (27 300), 677 (400).

Acknowledgements

We thank the Japan Society for the Promotion of Science for the research fellowship granted to D. C. O. We thank Miss Mie Tomonou of the Chemistry Department for the measurement of mass spectra.

References

1 For reviews see: (*a*) H. Iwamura, *Adv. Phys. Org. Chem.*, 1990, **26**, 179; (*b*) D. A. Dougherty, *Acc. Chem. Res.*, 1991, **24**, 88; (*c*) O. Kahn, *Molecular Magnetism*, VCH, New York, 1993; (*d*) H. Iwamura and N. Koga, *Acc. Chem. Res.*, 1993, **26**, 346; (*e*) H. Kurreck, *Angew. Chem., Int. Ed. Engl.*, 1993, **32**, 1409; (*f*) J. S. Miller and A. J. Epstein, *Angew. Chem., Int. Ed. Engl.*, 1994, **33**, 385; (*g*) A. Rajca, *Chem. Rev.*, 1994, **94**, 871; (*h*) G. Allinson, R. J. Bushby and J.-L. Paillaud, unpublished results.

2 (*a*) N. Nakamura, K. Inoue and H. Iwamura, *Angew. Chem., Int. Ed. Engl.*, 1993, **32**, 872; (*b*) K. Matsuda, N. Nakamura, K. Takahashi, K. Inoue, N. Koga and H. Iwamura, *J. Am. Chem. Soc.*, 1995, **117**, 5550.

3 (*a*) C. Benelli, A. Dei, D. Gattesci, H. U. Gudel and L. Pardi, *Inorg. Chem.*, 1989, **28**, 3089; (*b*) K. Inoue and H. Iwamura, *J. Am. Chem. Soc.*, 1994, **116**, 3173; (*c*) K. Inoue, T. Hayamizu and H. Iwamura, *J. Am. Chem. Soc.*, 1996, **118**, 1803.

4 K. Inoue and H. Iwamura, *J. Chem. Soc., Chem. Commun.*, 1994, 2273.

5 G. L. Davies and D. H. Hey, *J. Chem. Soc.*, 1956, 4397.

6 A. E. Tschitschibabin, *Ber. Dtsch. Chem. Ges.*, 1911, **44**, 450.

7 T. Sakai, K. Miyata, M. Utaka and A. Takeda, *Tetrahedron Lett.*, 1987, **28**, 3817.

8 As a reference for the generation of tris-lithio compounds, see G. J. Chen and C. Tamborski, *J. Organomet. Chem.*, 1983, **251**, 149.

9 T. Ishida, Ph.D. Thesis, the University of Tokyo, 1991.

10 (*a*) G. R. Luckhurst, *Mol. Phys.*, 1966, **10**, 543; (*b*) P. Michon and A. Rassat, *J. Am. Chem. Soc.*, 1975, **97**, 696.

11 F. Kanno, K. Inoue, N. Koga and H. Iwamura, *J. Phys. Chem.*, 1993, **97**, 13 267.

12 C. J. Pedersen, *J. Org. Chem.*, 1957, **22**, 2295.

13 T. Matsumoto, T. Ishida, N. Koga and H. Iwamura, *J. Am. Chem. Soc.*, 1992, **114**, 9952.

14 (*a*) N. C. Yang and A. J. Castro, *J. Am. Chem. Soc.*, 1960, **82**, 6208; (*b*) K. Mukai, K. Ishizu, M. Nakahara and Y. Deguchi, *Bull. Chem. Soc. Jpn.*, 1980, **53**, 3363; (*c*) H. van Willigen, B. Kirste, H. Kurreck and M. Plato *Tetrahedron*, 1982, **38**, 759; (*d*) H. Bock, A. John, Z. Havlas and J. W. Bats, *Angew. Chem., Int. Ed. Engl.*, 1993, **32**, 416.

15 B. Kirste, A. Krüger and H. Kurreck, *J. Am. Chem. Soc.*, 1982, **104**, 3850.

Paper 5/06285C
Received 22nd *September* 1995
Accepted 16th *November* 1995